JBC RESEARCH ARTICLE

Suppressed ORAI1-STIM1-dependent Ca^{2+} entry by protein kinase C isoforms regulating platelet procoagulant activity

Received for publication, February 13, 2024, and in revised form, October 9, 2024 Published, Papers in Press, October 17, 2024,
https://doi.org/10.1016/j.jbc.2024.107899

Jinmi Zou[1,2,‡], Pengyu Zhang[2,3,4,‡], Fiorella A. Solari[4,‡], Claudia Schönichen[2,3], Isabella Provenzale[2], Nadine J. A. Mattheij[5], Marijke J. E. Kuijpers[2], Julia S. Rauch[4], Frauke Swieringa[1], Albert Sickmann[4,6,7], Barbara Zieger[8], Kerstin Jurk[3], and Johan W. M. Heemskerk[1,2,*]

From the [1]Synapse Research Institute Maastricht, Maastricht, The Netherlands; [2]Department of Biochemistry, CARIM, 6200 MD Maastricht University, Maastricht, The Netherlands; [3]Center for Thrombosis and Hemostasis (CTH), University Medical Center of the Johannes Gutenberg University Mainz, Mainz, Germany; [4]Leibniz-Institut für Analytische Wissenschaften-ISAS-e.V, Dortmund, Germany; [5]Department of Clinical Chemistry and Hematology, Maxima Medical Center Veldhoven, Veldhoven, The Netherlands; [6]Medizinische Fakultät, Medizinische Proteom-Center, Ruhr-Universität Bochum, Bochum, Germany; [7]Department of Chemistry, College of Physical Sciences, University of Aberdeen, Aberdeen, United Kingdom; [8]Department of Pediatrics and Adolescent Medicine, Division of Pediatric Hematology and Oncology, Medical Center, University of Freiburg, Freiburg, Germany

Reviewed by members of the JBC Editorial Board. Edited by Mike Shipston

Agonist-induced rises in cytosolic Ca^{2+} control most platelet responses in thrombosis and hemostasis. In human platelets, we earlier demonstrated that the ORAI1-STIM1 pathway is a major component of extracellular Ca^{2+} entry, in particular when induced *via* the ITAM-linked collagen receptor, glycoprotein VI (GPVI). In the present article, using functionally defective platelets from patients with a loss-of-function mutation in *ORAI1* or *STIM1*, we show that Ca^{2+} entry induced by the endoplasmic reticulum ATPase inhibitor, thapsigargin, fully relies on this pathway. We demonstrate that both the GPVI-induced and thapsigargin-induced Ca^{2+} entry are strongly suppressed by protein kinase C (PKC) activation while leaving intracellular Ca^{2+} mobilization unchanged. Comparing the effects of a PKC inhibitory panel pointed to redundant roles of beta and theta PKC isoforms in Ca^{2+}-entry suppression. In contrast, tyrosine kinases positively regulated GPVI-induced Ca^{2+} entry and mobilization. Label-free and stable isotope phosphoproteome analysis of GPVI-stimulated platelets suggested a regulatory role of bridging integrator-2 (BIN2), known as an important mediator of the ORAI1-STIM1 pathway in mouse platelets. Identified were 25 to 45 regulated phospho-sites in BIN2 and 16 to 18 in STIM1. Five of these were characterized as direct substrates of the expressed PKC isoforms alpha, beta delta, and theta. Functional platelet testing indicated that the downregulation of Ca^{2+} entry by PKC resulted in suppressed phosphatidylserine exposure and plasmatic thrombin generation. Conclusively, our results indicate that in platelets multiple PKC isoforms constrain the store-regulated Ca^{2+} entry *via* ORAI1-BIN2-STIM1, and hence downregulate platelet-dependent coagulation.

Earlier research with bone-marrow transplanted chimeric mice (1, 2), platelets from immune-deficient patients (3) and pharmacological agents (4, 5) has indicated that the Ca^{2+} channel ORAI1 (CRACM1) operates as the main Ca^{2+} entry pathway in platelets. While in platelets and other cells, it is established that the ORAI1 channel is activated upon coupling to the STIM1 Ca^{2+} sensor in the endoplasmic reticulum (6), recent studies provide evidence that this coupling in mouse platelets involves the adaptor protein BIN2 (bridging integrator 2) (7). Thus, murine BIN2 links STIM1 to the reticular inositol 1,4,5-triphosphate (IP_3) receptors and thereby supports Ca^{2+} release from intracellular stores and ensuing store-operated Ca^{2+} entry (SOCE) *via* ORAI1. In platelets, SOCE is active in response to most receptor agonists and enhances the agonist-induced rises in cytosolic $[Ca^{2+}]_i$. The elevated $[Ca^{2+}]_i$ promotes most platelet responses, including shape change, granule secretion, thromboxane A_2 release, and platelet aggregation. In particular, SOCE is essential for Ca^{2+}-dependent surface exposure of phosphatidylserine and thereby for platelet procoagulant activity (8, 9).

The clinical importance of the ORAI1-STIM1 pathway appears from functional defects that are observed in platelets from patients with a pathological mutation in ORAI1 (R91W) or in STIM1 (R429C) (10, 11). These defects are accompanied by a severe immune deficiency due to compromised T-cell functions (12, 13). In contrast, patients with the autosomal inherited Stormorken syndrome, who carry gain-of-function mutations in ORAI1 or STIM1, present with increased platelet activation, leading to secondary thrombocytopenia and a bleeding diathesis (14, 15). In mouse, the deletion of platelet ORAI1 or STIM1 suppresses platelet activation and down-regulates pathological arterial thrombus formation (1, 2). These studies hence imply that the SOCE pathway is well-controlled to prevent platelet under- or over-activation and to ensure a proper hemostatic balance. Mouse studies suppose that also in humans the BIN2 adaptor protein regulates ORAI1-STIM1 dependent Ca^{2+} entry.

Recent high-throughput well-plate measurements of platelet $[Ca^{2+}]i$ rises, using a panel of pharmacological inhibitors,

‡ These authors have contributed equally to this work.
* For correspondence: Johan W. M. Heemskerk, jwmheem722@outlook.com.

confirmed that the ORAI1-STIM1 axis is a major route for Ca^{2+} entry in human platelets (16). This was true for platelets stimulated *via* the protein tyrosine kinase-linked receptor for collagen glycoprotein VI (GPVI) and *via* the protease-activated thrombin receptors PAR1 and PAR4. Both receptor types act through activation of protein kinase C (PKC) isoforms (17). Structurally, these are separated into the conventional PKC (cPKC) isoforms (α, β, and γ) with Ca^{2+} and diacylglycerol binding sites, the novel PKC (nPKC) isoforms (δ, ε, η, and θ) with only a diacylglycerol-binding domain and the atypical isoforms (ζ and ι/λ) acting independently of Ca^{2+} and diacylglycerol. Well expressed in human platelets are the cPKC isoforms PKCα and PKCβ and the nPKC isoforms PKCδ, PKCθ, and PKCη (Table 1) (18).

Whereas the platelet thrombin receptors PAR1 and PAR4 as G protein-coupled receptors act *via* Gq and conventional downstream signaling events, the ITAM-linked receptor GPVI signals *via* the protein tyrosine kinase cascade, involving Src-family kinases, Syk and Btk (8, 9). Where the PARs induce transient $[Ca^{2+}]_i$ rises in platelets, GPVI stimulation causes a more persistent $[Ca^{2+}]_i$ elevation, which is still not well understood (3, 9).

It is generally considered that in human and mouse platelets cPKC and nPKC isoforms jointly regulate integrin activation and aggregation (19, 20). However, paradoxical results exist regarding the roles of PKC isoforms in platelet Ca^{2+} signaling. In mouse platelets, collagen-induced $[Ca^{2+}]$i rises were downregulated upon deficiency of PKCα or PKCβ, and enhanced upon deficiency of PKCθ but not PKCη (21). In human platelets, inhibition of total PKC or nPKC isoforms appeared to increase the $[Ca^{2+}]_i$ rises with collagen and other agonists (21, 22). A complicating factor is that PKC-dependent phosphorylation was found to interfere with GPVI-induced phosphorylation of the tyrosine kinases Syk and Btk (23, 24). If and how SOCE *via* ORAI1 channels can separately be regulated by PKC isoform activities is still unknown.

In this study, we employed the high-throughput assay for measurements of Ca^{2+} responses in human platelets (25) to elucidate the roles of PKC isoforms in the SOCE process, mediated by the ORAI1, BIN2, and STIM1 pathways. We studied platelets from patients with index mutations in *ORAI1* or *STIM1* to define activation conditions relying on this pathway, and we performed two platelet phospho-proteome analyses to identify PKC isoform-sensitive phosphorylation regions in BIN2 and STIM1. Platelet procoagulant activity was used as a functional test relying on high Ca^{2+} rises.

Results

Suppression of GPVI-induced platelet Ca^{2+} entry by Btk and low cPKC inhibition

To systematically investigate the roles of protein kinases in agonist-induced platelet Ca^{2+} responses, we used human Fura-2-loaded platelets and a previously standardized 96-well plate assay, in which agonists are added at high throughput by robotic injection (25). For discriminating between Ca^{2+} entry *via* SOCE and Ca^{2+} mobilization from intracellular stores, the platelets were stimulated in the presence of either 2 mM CaCl2 or 0.1 mM EGTA with near-maximal stimulating doses of the GPVI agonists, convulxin (50 ng/ml) or CRP (5 μg/ml) (16).

Preincubation of the platelets with Btk inhibitor acalabrutinib (0.3–10 μM) resulted in a dose-dependent inhibition of peak and end-level $[Ca^{2+}]$i rises in response to convulxin, regardless of the presence of CaCl2 or EGTA (Fig. 1, *A–D*). At the highest dose of 10 μM, acalabrutinib essentially abolished the effects of convulxin. When platelets were stimulated with CRP, as a slowly acting crosslinked triple-helical peptide requiring interactions with several GPVI molecules (16), acalabrutinib (0.3–10 μM) similarly suppressed the $[Ca^{2+}]$i peak and end levels (Fig. S1, *A* and *B*). These data are in line with the established tyrosine kinase-dependent mode of action of GPV agonists and furthermore show that the kinase Btk next to Syk is essential for the Ca^{2+} response generation.

Different effects were obtained with the inhibitor Gö6976 (0.3–10 μM). This compound inhibits PKC isoforms α, β, η and to a lesser extent PCK δ and θ (Table 1). Gö6976 has also been shown to inhibit Syk activity (26). In contrast to the lowest dose of 0.3 μM, Gö6976 caused at higher concentrations a significant decrease in the convulxin-induced $[Ca^{2+}]$i rises (Fig. 2, *A* and *B*). At ≥1 μM, it suppressed the Ca^{2+} signal

Table 1
Characteristics of platelet PKC isoforms and inhibitors

	PKCα	PKCβ	PKCδ	PKCη	PKCθ	Ref
Copy number						
Per platelet	7882	9774	6217	3871	668	(18)
Residual activity (%)						
GF109203X	6	8	5	17	7	(43)
Gö6976	8	14	42	7	35	(43)
PKCβ-IN	99	21	98	83	98	(43)
Inhibitory strength						
RO31318425 (10)	++	++	++	++	++	(21)
PKCθ-IN (1)	o	o	o	+	++	(21)
Predicted phosphorylation (PhosphoSite)						
BIN2 T285	+	+	+	+	+	(32)
BIN2 S429/430	+	+	+	-	-	(32)
BIN2 T446/S451	+	+	+	-	+	(32)
STIM1 S512	+	+	+	-	-	(32)

Indicated are reported copy numbers per platelet, residual activity in high-throughput comparisons. Note that compounds were tested in Ref. 43 on isolated enzymes at 10 μM ATP and 0.5 μM, which requires higher concentrations when applied to intact cells. Furthermore indicated is relative inhibitory strength at indicated concentration (μM), as reported in Ref. 21. Bottom part gives predicted role in phosphorylation of BIN2 and STIM1 serines/threonines, based on submitted phosphopeptides, obtained from our platelet proteome analysis.

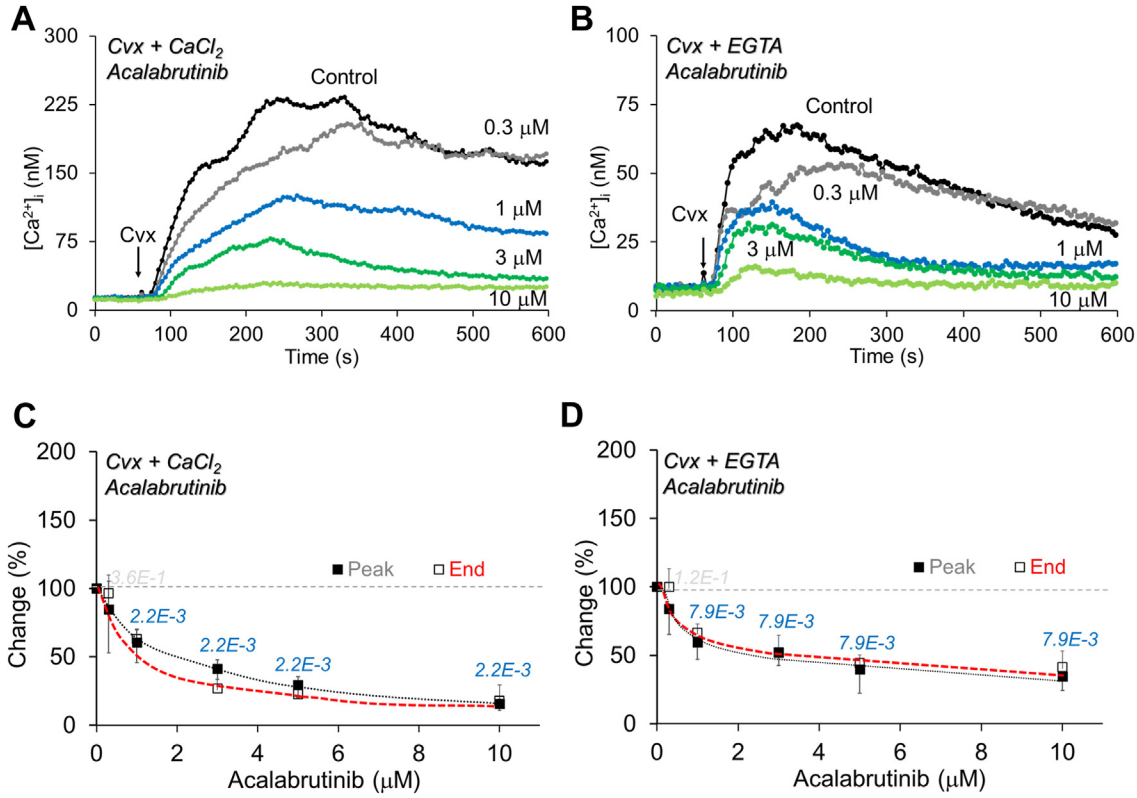

Figure 1. Suppression of convulxin-induced platelet Ca^{2+} responses by Btk inhibitor acalabrutinib. Fura-2-loaded platelets in 96-well plates were preincubated with DMSO vehicle or acalabrutinib (0.3–10 μM) for 10 min at 37 °C, and stimulated with convulxin (Cvx, 50 ng/ml) in the presence of 2 mM CaCl2 or 0.1 mM EGTA. Ratio fluorometric measurements were converted into calibrated nM levels of $[Ca^{2+}]i$. Convulxin was injected at the indicated time and activated the platelets in a diffusion-limited way. *A–B*, representative $[Ca^{2+}]i$ traces upon stimulation with convulxin with CaCl2 (*left*) or EGTA (*right*). *C–D*, Dose-dependent effect of acalabrutinib on $[Ca^{2+}]i$ peak and end levels. Given are percentage changes *versus* control condition (vehicle medium). Mean ± SD (n = 4–6), significant *p*-values vs. control condition for peak levels in *blue* (Mann-Whitney U test).

over time to about 50% in the presence of CaCl2, but insignificantly in the presence of EGTA (Fig. 2, *C* and *D*). Also for the slower-onset GPVI agonist CRP, Gö6976 dose-dependently suppressed the Ca^{2+} response (Fig. S2, *A* and *B*). When compared to acalabrutinib (Fig. 1), the higher, but not lower dose effects of Gö6976 resembled those of Btk inhibition. The former can thus be explained by the off-target effect of Syk inhibitor (26).

Enhancement of GPVI-induced platelet Ca^{2+} entry by pan-PKC and PKC isoform inhibition

To check for the cumulative role of PKC isoforms in platelet Ca^{2+} responses, we examined the effects of two pan-PKC inhibitors, namely GF109203X and RO318425, affecting cPKC and nPKC forms (Table 1). At concentrations of 0.3 to 3 μM, GF109203X caused a major, up to 4-fold enhancement of the Ca^{2+} response with convulxin + CaCl2, and a small later-in-time peak increase with EGTA (Fig. 3, *A–D*). However, at 10 μM, the enhancement was annulled. Similar, major enhancing effects at 0.3 to 3 μM were obtained with the GPVI agonist CRP + CaCl2 (Fig. S3). Along the same line, the pan-PKC inhibitor RO318425 enhanced the peak Ca^{2+} responses with convulxin or CRP up to 3-fold over the full dose range of 0.3 to 10 μM with extracellular CaCl2 present (Fig. S4). The Ca^{2+}-signal potentiating effect of both inhibitors, though biphasic at a high GF109203X dose, pointed to a strong PKC-dependent suppression of GPVI-induced Ca^{2+} entry. Being distinct from the suppressive effect of acalabrutinib, we concluded that the CaCl2-dependent potentiation by overall PKC inhibition was disconnected from the Btk-Syk pathway.

Subsequently, we compared the effects of several PKC isoform-selective inhibitors (Table 1) on Ca^{2+} entry responses induced by the common GPVI agonist CRP + CaCl2 (Fig. S5). At optimally effective concentrations, PKCβ- or PKCθ-directed inhibition with PKCβ-IN or PKCθ-IN caused Ca^{2+} peak increases of 2.41 ± 0.26 fold (mean ± SD, p = 0.03) or 1.38 ± 029 fold (p = 0.09), respectively, which though were lower than the 3.5 to 3.8 fold enhancement obtained with pan-PKC inhibitors GFX109203X and RO318425. In contrast, maximal PKC stimulation with PMA together with CRP resulted in a reduced, 0.70 ± 0.11 fold (p = 0.03) Ca^{2+} peak level (Fig. S5). Together, this suggested a contribution of at least two PKC isoforms in the suppression of Ca^{2+} entry.

When testing this regulation with TRAP6 (PAR1 agonist) or thrombin (PAR1/4 agonist) + CaCl2, the pan-PKC inhibitor RO318425 caused moderate enhancing effects, while PMA essentially abolished the Ca^{2+} response (Fig. S6). This indicates

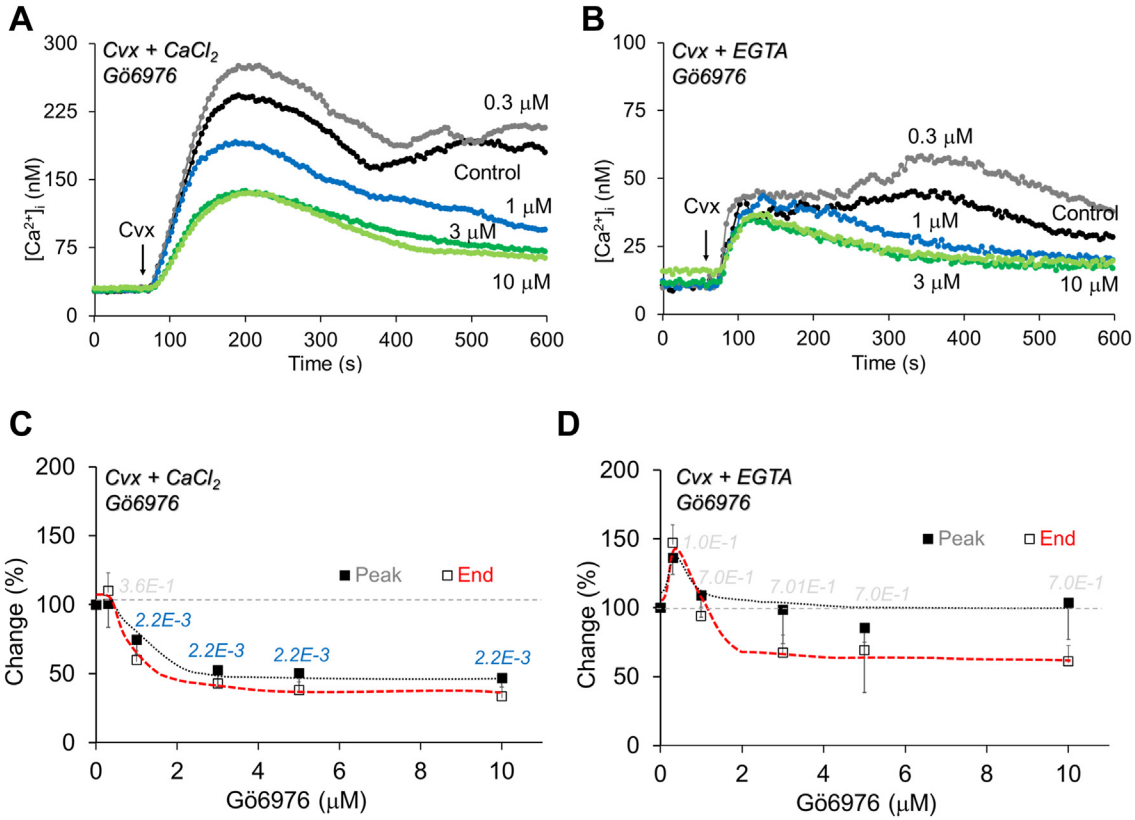

Figure 2. Low-dose enhancement convulxin-induced platelet Ca^{2+} responses by compound Gö6976. Fura-2-loaded platelets were preincubated with DMSO control medium or Gö6976 (0.3–10 µM) for 10 min at 37 °C, and stimulated with convulxin (50 ng/ml) or CRP (5 µg/ml) in the presence of 2 mM $CaCl_2$ or 0.1 mM EGTA. Data were collected as for Fig. 1. *A–B*, representative $[Ca^{2+}]$i traces with CaCl2 (*left*) or EGTA (*right*). *C–D*, Dose-dependent effect of Gö6976 on $[Ca^{2+}]$i peak and end levels (change *vs.* 100% of control). Mean ± SD (n = 3–6), significant *p*-values vs. control condition for peak levels in *blue* (Mann-Whitney U test).

a submaximal PKC stimulation by agonists and agrees with a lower contribution of SOCE to the Ca^{2+} signal of PAR stimulation in comparison to GPVI (16).

Role of PKC isoforms in platelet SOCE regulation via *ORAI1-STIM1*

In platelets, the SERCA inhibitor, thapsigargin causes long-term Ca^{2+} store depletion (27). To confirm a key role of the ORAI1-STIM1 Ca^{2+} entry pathway after thapsigargin treatment, we studied the platelets from patients with a genetic defect in ORAI1 (homozygous R91W) or STIM1 (heterozygous R429C). Both mutations are known to result in protein dysfunction (11).

With platelets from healthy control subjects, CaCl2 addition after thapsigargin resulted in a strong $[Ca^{2+}]$i increase, reaching micromolar levels (Fig. 4, *A* and *B*). Strikingly, after thapsigargin treatment of platelets from both patients, the response to CaCl2 addition was essentially lost (Fig. 4, *A–D*). Furthermore, in the patient platelets, the response to CaCl2 after convulxin stimulation was partly (ORAI1 R91W) or slightly (STIM1 R429C) impaired. From these results, we concluded that the thapsigargin + CaCl2 protocol provided a suitable way to quantify the ORAI1-STIM1 pathway in platelets.

Using platelets from healthy subjects, we then found that pretreatment with the pan-PKC inhibitors GF109203X or RO318425 resulted in an additional increase in $[Ca^{2+}]$i in response to thapsigargin + CaCl2, raising the concentration to as high as 8 to 10 µM (Fig. 5*A*). In sharp contrast, platelet pretreatment with the pan-PKC stimulus PMA strongly reduced the Ca^{2+} entry to ~1 µM. A similar reduction was seen with the ORAI1-channel inhibitor 2-APB (Fig. 5*B*). However, platelet pretreatment with the PKC isoform inhibitors PKCθ-IN or Gö6976 did not affect the level of $[Ca^{2+}]$i in response to thapsigargin + CaCl2. Control experiments indicated that the compounds did not influence the low Ca^{2+} signal in the absence of thapsigargin (Fig. 5*C*).

Quantification of normalized Ca^{2+}-time traces indicated a 30 to 40% Ca^{2+} entry increase (at 10 min) with the two pan-PKC inhibitors, but no increase or rather a reduction with Gö6976, PKCθ-IN or PKCβ-IN (Fig. 5*D*). Furthermore, the suppressed Ca^{2+} entry signal by PMA was restored by the simultaneous addition of PKCβ-IN > PKCθ-IN. These data hence suggested that the low PKC stimulation with thapsigargin is substantially increased with PMA, then inducing a potent constrain of the Ca^{2+} entry due to Ca^{2+} store depletion. The partial reversal effects by PKCβ or PKCθ inhibition with PMA present pointed to a role of at least these two isoforms in the suppression of SOCE. Our data further agree with the

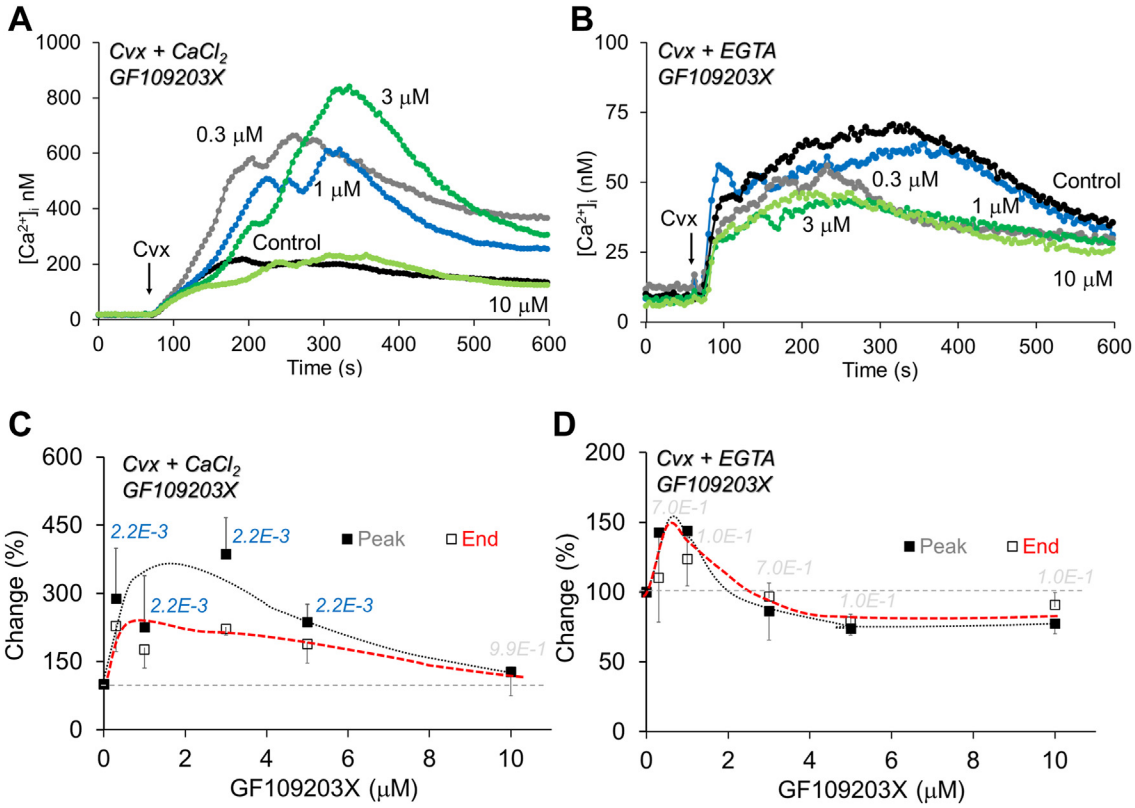

Figure 3. Enhancement on convulxin-induced Ca^{2+} entry by pan-PKC inhibitor GF109203X. Fura-2-loaded platelets were preincubated with DMSO control medium or GF109203X (0.3–10 μM) for 10 min at 37 °C, and stimulated with convulxin (50 ng/ml) in the presence of 2 mM CaCl2 or 0.1 mM EGTA. See further Fig. 1. *A–B*, representative $[Ca^{2+}]$i traces with CaCl2 (*left*) or EGTA (*right*). *C–D*, dose-dependent effect of GF109203X on $[Ca^{2+}]$i peak and end levels (change *vs.* 100% of control). Mean ± SD (n = 3–6), significant *p*-values vs. control condition for peak levels in *blue* (Mann-Whitney U test).

established role of ORAI1- STIM1-mediated SOCE in platelet activation (16).

PKC-induced suppression of platelet procoagulant activity and thrombin generation

To assess for functional effects of the PKC-dependent suppression of Ca^{2+} entry, we assessed platelet responses that are known to rely on consistently high levels of $[Ca^{2+}]$i, namely agonist-induced externalization of the procoagulant phospholipid phosphatidylserine (28, 29), and the phosphatidylserine-dependent amplification of thrombin generation, marking the coagulation process (30). Therefore, we treated platelets with a panel of PKC inhibitors and monitored convulxin-induced phosphatidylserine exposure by flow cytometry. Pan-PKC inhibition with GF109203X or RO318425 increased the phosphatidylserine exposure from 17% to over 50 to 57% of the platelet population (Fig. 6*A*, histograms in Fig. S7). Treatment with PKCθ- IN, but not Gö6976, also increased phosphatidylserine exposure. On the other hand, platelet treatment with pan-PKC activator PMA substantially reduced the phosphatidylserine exposure to <10% (Fig. 6).

In addition, we measured the consequences of PKC modulation on thrombin generation in tissue factor-triggered platelet-rich plasma, as a phosphatidylserine-dependent process (30). In agreement with the flow cytometry data, pretreatment with GF109203X or RO318425 increased the measured thrombin peak levels in a dose-dependent way to over 2-fold (Fig. 6, *B* and *C*). In contrast, pre-stimulation of PKC with PMA left thrombin peak levels unchanged, but shortened the lag-time to thrombin generation (Fig. 6, *D* and *E*), which is explained by the secretion-stimulating effect of PKC, releasing coagulation factor V.

Altered serine/threonine phosphorylation of BIN2 and STIM1 in GPVI- and PAR-activated platelets

We then used proteomic approaches to find evidence on the protein phosphorylation level for PKC-dependent modulation of the ORAI1-BIN2-STIM1 pathway. For this purpose, platelets from three healthy donors were stimulated with CRP + CaCl2 (3 min) or thrombin + CaCl2 (30 s). The stimulation times were chosen to give maximal $[Ca^{2+}]$i rises, as checked in parallel Ca^{2+} measurements. After lysis, the platelet samples were subjected to controlled trypsin digestion and a label-free bottom-up phospho-proteome analysis, in order to generate maximal numbers of phosphopeptides (31). For BIN2 as many as 249 phospho-peptides were obtained with 1 to 4 phosphorylations (Datafile S1). The phospho-peptides covered 45 different serines or threonines, which were mostly located before and in four polar regions (labeled *pre-a*, *a-d*) of amino acid residues 257 to 508 (Fig. 7*A*). Structurally, polar regions are commonly found at a protein's contour. Calculation of the mean log2-fold changes per phospho-site indicated a pattern

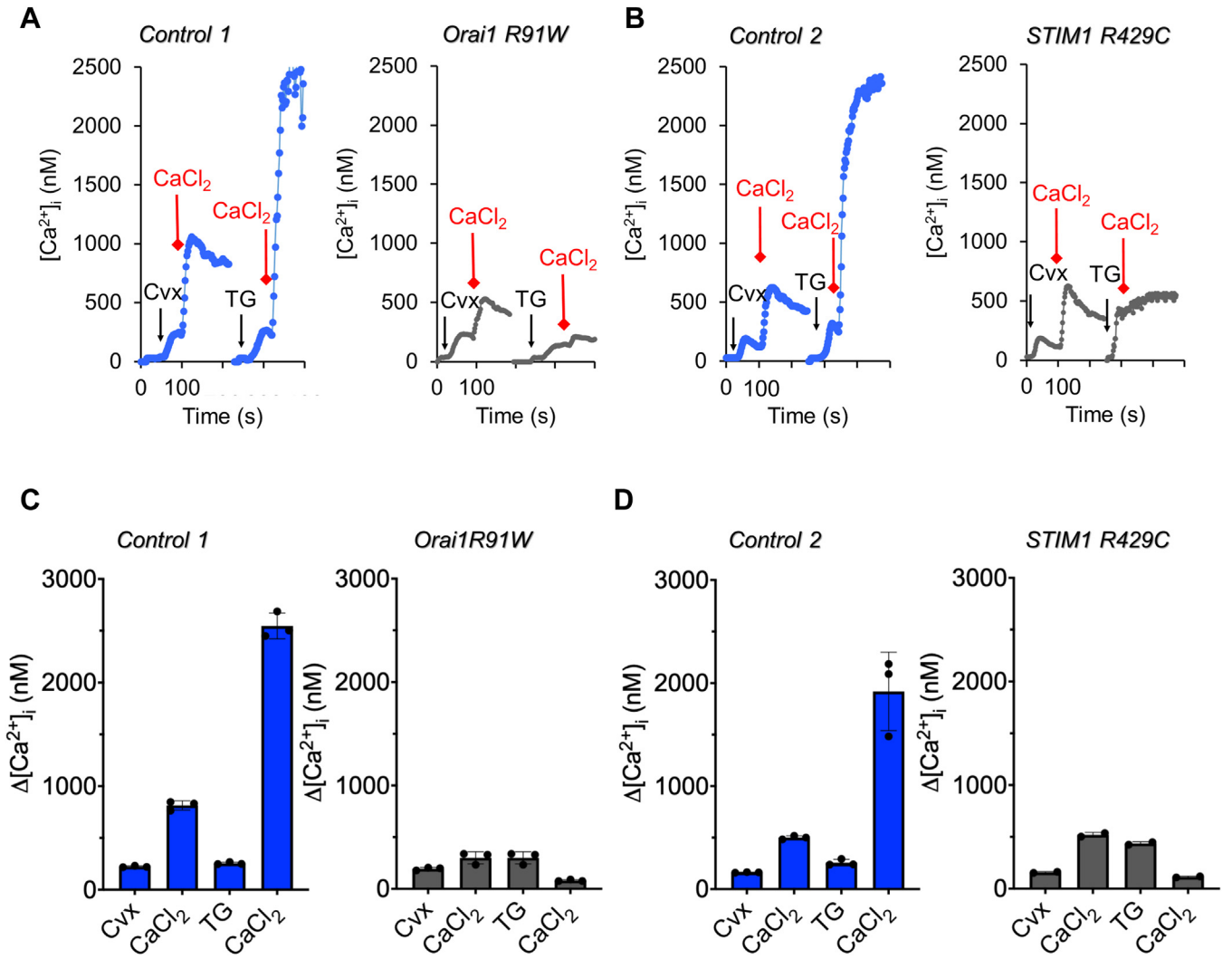

Figure 4. Impaired Ca^{2+} entry in platelets from patients with a dysfunctional mutation of *ORAI1* or *STIM1*. Fura-2-loaded platelets (2×10^8/ml) in 0.1 mM EGTA medium from indicated patients or day control subjects in cuvettes were triggered with 50 ng/ml convulxin (Cvx), followed by 2 mM CaCl2. Alternatively, the platelets were triggered with 1 μM thapsigargin (TG), followed by 2 mM CaCl2. *A*, representative $[Ca^{2+}]$i traces of platelets from control subject-1 and patient ORAI1 R91W (homozygous). *B*, representative $[Ca^{2+}]$i traces of platelets from control subject-2 and patient STIM1 R429C (heterozygous). *C–D*, quantification of peak increases in $[Ca^{2+}]$i. Data are mean ± SD (n = 2–3 repeats).

of clusters in these regions, with agonist-induced changes that were similar in platelets of the three donors. After CRP or thrombin stimulation, the phospho-sites in the *pre-a*, *a*, and *b* regions (S259-S381) were significantly increased (Fig. 7, *B* and *C*). Regarding regions *c* + *d*, the results for CRP were more complex with specific phospho-site increases in *c* (S429, S451) and *d* (T497, S498).

For STIM1, we identified 18 different phospho-sites that were all located in serine-rich cytoplasmic domains *a* + *b* of the protein (Fig. S8*A*). Platelet stimulation with CRP more than thrombin caused an increase in phosphorylations at residues 512 to 528 (*a*), and stimulation with thrombin a decrease at residues 595 to 626 (*b*) (Fig. S8, *B* and *C*). For the relatively small ORAI1 protein, the only observed phospho-sites in cytoplasmic residues 295 to 298 were not regulated (Fig. S8*D*).

These proteomic results indicated extensive, previously unknown serine/threonine phosphorylation of BIN2 in platelets stimulated *via* GPVI or PAR. This is in line with data, indicating that BIN2 in mouse platelets regulates the functions of STIM1 and SOCE (7). To identify PKC-dependent phosphorylations, all obtained phospho-peptides were checked against the database PhosphoSite-Plus, predicting substrate sites for 303 serine/threonine kinases (32).

The analysis resulted for BIN2 in three predicted PKC isoform-dependent phosphorylations, namely S285 (PKCαβδηθ), S429/S430 (PKCαβδ) and S451/S458 (PKCαβδ) (Datafile S1). Interestingly, we found for all three sites increased CRP-induced phosphorylation, *i.e.* 1.06 ± 0.74 (mean ± SD, n = 3; p = 0.009), 0.64 ± 0.23 (p = 0.039) and 1.58 ± 0.25 (p = 0.008), respectively (Fig. 7*B*). Regarding the STIM1 protein, S512 showed a strong positive prediction as a substrate for PKCαβδηθ isoforms. The CRP-induced increase in phosphorylation at this site was significant at 2.55 ± 1.21 (p = 0.034) (Fig. S6*B*).

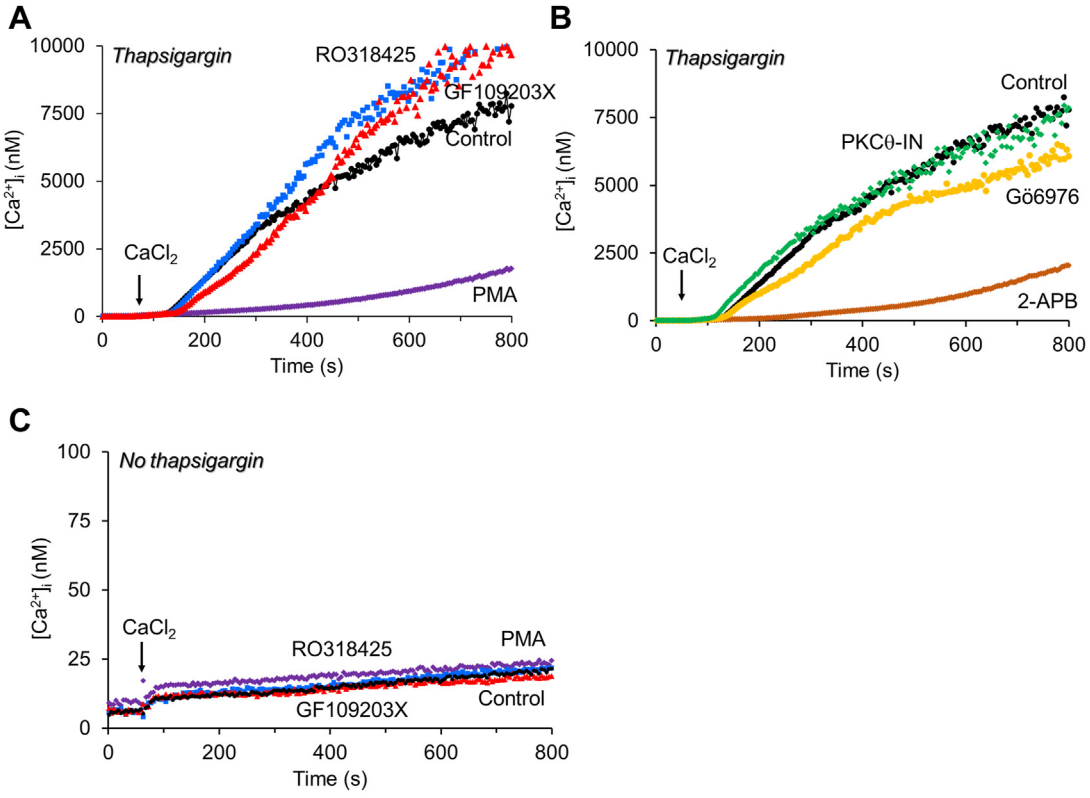

D

Thapsigargin + $CaCl_2$ (n=3-6)

Mean

Time (s)	50	200	400	600	800	N
Control	0.2	18.2	58.9	100.0	128.5	6
GF109203X	0.3	5.6	44.8	143.9	190.9	5
RO318425	0.3	17.0	75.4	134.7	168.3	6
PKCθ-IN	0.3	16.4	65.7	97.2	133.0	6
Gö6976	0.1	10.4	40.7	63.2	81.6	4
PKCβ-IN	0.2	7.6	36.0	56.6	89.1	5
PMA	0.3	2.2	4.6	9.7	20.0	6
PMA + PKCθ-IN	0.4	5.3	12.1	26.6	51.3	4
PMA + PKCβ-IN	0.3	15.2	38.1	58.1	70.8	3

SD

Time (s)	50	200	400	600	800
Control	0.2	6.8	13.9	0.0	26.2
GF109203X	0.2	4.9	29.0	33.8	61.4
RO318425	0.3	16.9	33.8	33.4	53.4
PKCθ-IN	0.2	7.5	28.9	39.4	40.6
Gö6976	0.1	4.6	18.3	25.2	29.3
PKCβ-IN	0.2	4.1	17.1	27.5	24.2
PMA	0.2	1.4	2.3	4.6	8.0
PMA + PKCθ-IN	0.3	1.1	2.6	3.4	2.5
PMA + PKCβ-IN	0.0	6.4	17.3	15.2	11.9

P

50	200	400	600	800
0.762	*0.008*	*0.429*	*0.049*	*0.126*
0.623	*0.394*	*0.093*	*0.048*	*0.394*
0.937	*0.699*	*0.818*	*0.999*	*0.841*
0.510	*0.011*	*0.017*	*0.005*	*0.019*
0.931	*0.017*	*0.030*	*0.002*	*0.038*
0.563	*0.002*	*0.002*	*0.002*	*0.004*
0.476	*0.010*	*0.010*	*0.005*	*0.010*
0.548	*0.905*	*0.167*	*0.012*	*0.024*

Figure 5. Modulation by PKC of thapsigargin-mediated Ca^{2+} entry in platelets. Fura-2-loaded platelets in 96-well plates were pretreated for 10 min with vehicle (control) or optimized doses of PMA (50 nM), GF109203X (3 μM), RO318425 (10 μM), Gö6976 (1 μM), PKCθ-IN (3 μM) or 2-ABP (30 μM) in the presence of 0.1 mM EGTA. After the addition of 1 μM thapsigargin (*A–B*) or vehicle (*C*), fluorescence ratio changes were recorded in response to 2 mM CaCl2 (at 60 s). Shown are representative traces of changes in $[Ca^{2+}]$i with (*A-B*) or without (*C*) of thapsigargin. *D*, Normalized $[Ca^{2+}]$i values *versus* control condition at 600 s, set at 100% per donor. A peak level of $[Ca^{2+}]$i was 12.1 ± 6.7 μM (mean ± SD, n = 6 experiments). Heatmaps represent normalized means (*top*), SD (*bottom left*), and *p*-values (*bottom right*). Significant differences from the control condition are underlined (Mann-Whitney U test).

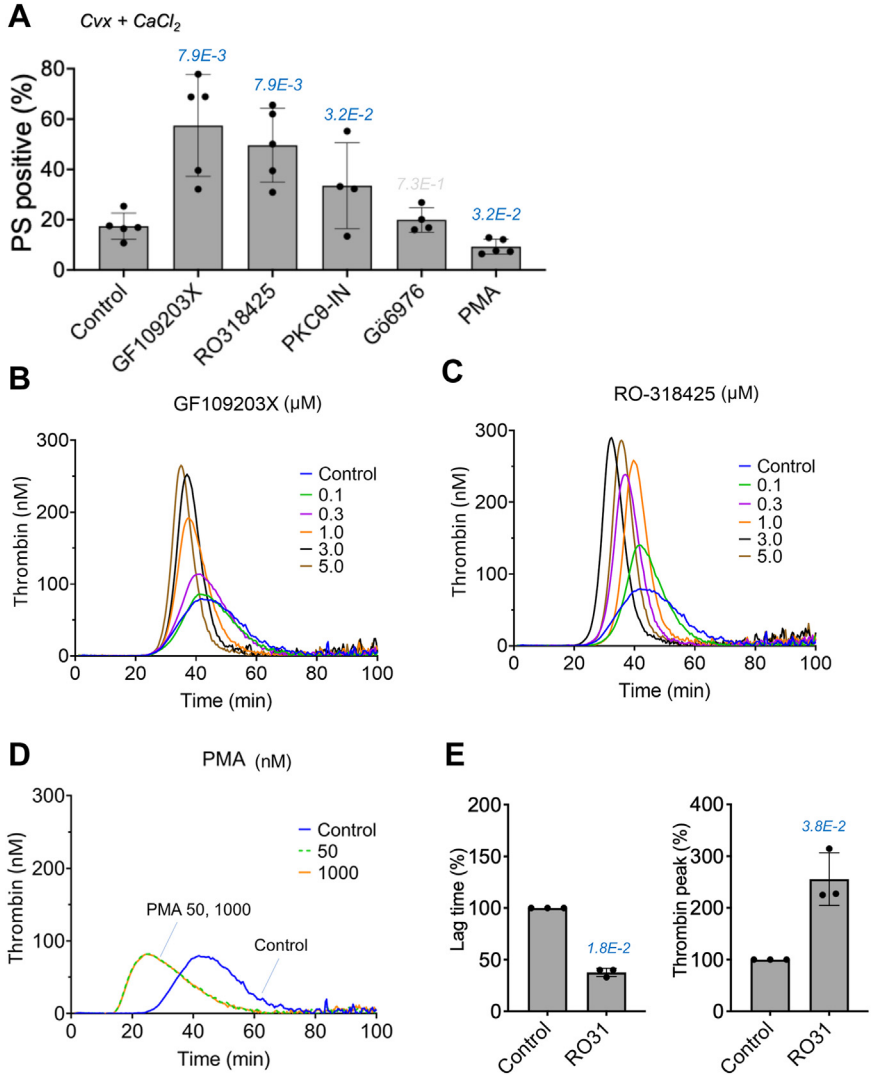

Figure 6. Modulation by PKC activity of platelet procoagulant activity and thrombin generation. *A*, washed platelets were pre-treated with DMSO control vehicle, GF109203X (3 μM), RO318425 (3 μM), PKCθ-IN (3 μM), Gö6976 (1 μM) or PMA (50 nM). The cells were then activated with convulxin (Cvx, 50 ng/ml) for 5 to 10 min in the presence of 2 mM CaCl2, labeled with FITC annexin A5 (0.25 μg/ml), and analyzed for phosphatidylserine (PS) expression. Shown are % of positive platelets after 10 min of stimulation; mean ± SD (n = 4–5); *p*-values vs. control condition in italics (Mann-Whitney U test). *B–E*, samples of PRP in 96-wells plates were incubated for 10 min DMSO control, GF109203X (0.1–5.0 μM), RO318425 (0.1–5.0 μM), or PMA (50–500 nM). Calibrated thrombin generation from cleaved Z-GGR-AMC substrate was measured per well upon triggering with 0.1 PM tissue factor in the presence of $CaCl_2$/$MgCl_2$. Shown are first-derivative thrombin generation curves representative of three experiments. *E*, normalized effect of RO318425 (3 μM) on thrombin lag time and thrombin peak level (mean ± SD, n = 3). *p*-values vs. control condition in italics.

To confirm these phosphorylation changes, we performed a second, independent phosphoproteome analysis, now assessing the short-term (as above) and long-term (30 min) effects of CRP and thrombin using tandem mass tag (TMT) labeling. For BIN2 this resulted in similar changes in 13 phospho-sites in regions *pre-a*, *a*, and *b*, often extending to 30 min of stimulation (Fig. S9, *A–C*). Most consistent were increased CRP- and thrombin-induced phosphorylations of predicted PKC isoform sites S256 (PKCαβδηθ) and S451 (region *c*, PKCαβ(δ)). Regarding STIM1, with 16 phospho-sites obtained, the data for S512 (PKCαβδηθ) showed an increased CRP- and thrombin-induced phosphorylation of 2.18 ± 0.73 and 1.55 ± 0.70, respectively (Fig. S10, *A–C*). Interestingly, STIM1 $Ser^{512}Gly$ is also recorded as a genetic variant (unknown significance) in ClinVar.

Given the important role of PKC isoforms proximal in the network of protein kinases and phosphatases in agonist-induced platelet activation, we concluded that hence speculate that multiple of the expressed αβδηθ isoforms, directly or indirectly, modulate the adaptor functions of BIN2 and STIM1 to interact with the ORAI1 channel in the plasma membrane.

Discussion

The present results provide the first evidence that several PKC isoforms, in particular PKCβ and PKCθ, in platelets exert a constraining effect on the entry of extracellular Ca^{2+} operating *via* the ORAI1-STIM1 pathway, and furthermore that this PKC activity downregulates GPVI-induced platelet procoagulant activity and thrombin generation. In the majority of Ca^{2+} measurements, the two pan-PKC inhibitors used

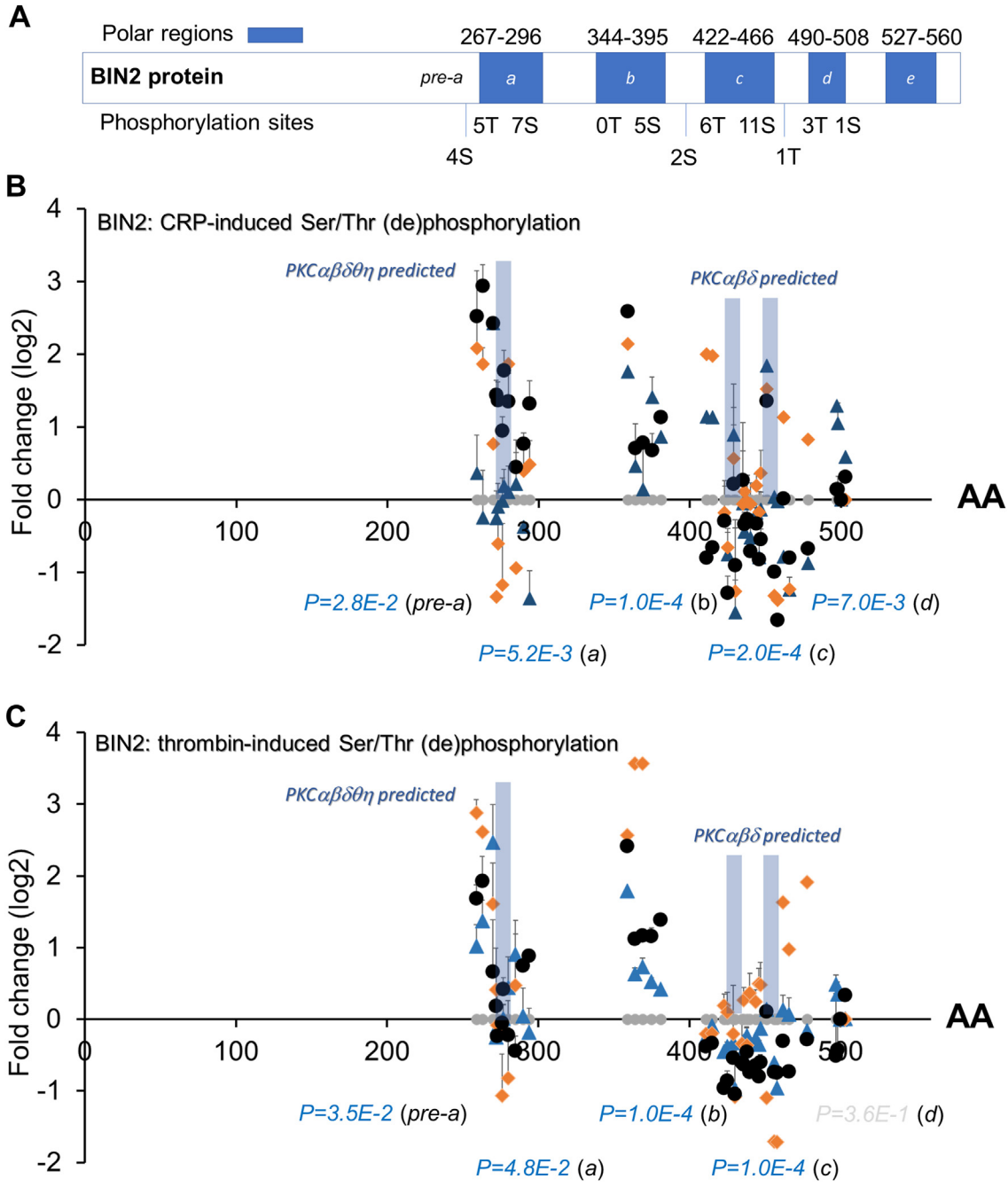

Figure 7. Alterations in BIN2 phosphorylation of platelets stimulated *via* GPVI or PAR1/4. Washed platelets from three donors (5×10^8/ml) in buffer containing 2 mM CaCl2 were stimulated with CRP (10 μg/ml, 3 min), with thrombin (4 nM, 30 s), or were *left* untreated. *Bottom-up* label-free phosphoproteome analysis was performed of the trypsin-treated platelet lysates. For BIN2, this provided quantitative information on 45 phospho-sites (regions in brackets): S257, S259, S263 (*pre-a*), T270, S272, S273, S276, S277, T279, S280, T283, S285, S288, S290, S294, T296 (*a*); S359, S364, S369, S375, S381 (*b*); S411, S415; T423, S425, S426, S429, S430, S435, S436, T438, S440, S444, T446, T447, S451, T456, S458, T462, S466 (*c*); T478; T497, S498, T500, T503 (*d*). *A*, overall structure of human BIN2 protein with five surface-exposed polar regions indicated in *blue*. Total numbers of phospho-sites of threonine (T) and serine (S) are indicated. *B*, CRP-induced log2 fold changes per phospho-site. Symbol types represent one donor; gray symbols are for unstimulated platelets. Data are shown as mean ± SD for all peptides with the same phospho-site. *C*, Idem, thrombin-induced log2 fold changes per phospho-site. Fold-changes, as compared to the control condition, for all donors were statistically evaluated per (pre)polar region, with *P*- values in italics (Mann-Whitney U-test). For S285, S429, and S451 with strong positive predictions as substrate for indicated PKC isoforms (see Table 1), CRP-induced fold-changes (mean ± SD) for three donors are: 1.06 ± 0.74 (p = 8.9E-3), 0.64 ± 0.23 (p = 3.9E-2), and 1.58 ± 0.25 (p = 8.2E-3), respectively. Full data in Datafile S1.

(GF109203X and RO318425) at maximally effective concentrations, had larger stimulating effects than the isoform-selective inhibitors (PKCβ-IN, PKCθ-IN, Gö6976). Conversely, additional PKC isoform stimulation with PMA reduced the platelet Ca^{2+} responses.

The observed defective Ca^{2+} entry with thapsigargin in platelets from patients with a loss-of-function mutation in *ORAI1* or *STIM1* indicated that the addition of CaCl2 after thapsigargin provides a suitable manner for assessment of the ORAI1-STIM1 pathway. In the patients' platelets, the CaCl2-

induced rises in [Ca^{2+}]i were fully abolished, such in contrast to the micromolar rises with platelets from control subjects. In the control platelets, we observed that both the pan-PKC stimulus PMA and the SOCE blocker 2-APB nearly completely suppressed the Ca^{2+} entry after thapsigargin treatment. The effects of PKCβ and PKCθ inhibitors, each partly antagonizing the suppression by PMA, indicated that at least these two isoforms contribute to the PKC- dependent suppression of GPVI-induced Ca^{2+} entry. In contrast, we found that the tyrosine kinase Btk promoted this pathway. In GPVI-stimulated platelets, the compound Gö6976 was inhibitory, which is explained by an off-target effect as inhibitor of the tyrosine kinase Syk (26).

Searching for a contribution of the adapter protein BIN2, we performed a label-free and stable isotope phospho-proteomic analysis of GPVI- and PAR-stimulated platelets, which identified 25 to 45 regulated phospho-sites in BIN2 and 16 to 18 in STIM1, clustered in serine/threonine-rich intracellular domains of the proteins. Four of these showed a strong positive prediction as substrates for PKC isoforms, partly for PKCαβδηθ and partly for PKCαβδ. Interestingly, no such phospho-sites were found for the channel protein ORAI1. Collectively, from these findings, we concluded that in human platelets protein phosphorylation *via* PKC isoforms provides a strong negative feedback mechanism of the store-regulated Ca^{2+} entry pathway *via* the ORAI1-BIN2- STIM1 axis, downregulating platelet procoagulant activity and platelet-dependent coagulation.

Recent mouse knockout studies have identified BIN2 as an important adaptor protein linking platelet IP3 receptors with the Ca^{2+}-store sensor STIM1 and thereby supporting the SOCE mechanism (7). For human platelets, this adaptor role of BIN2 is not confirmed, but our results strongly support the mouse experiments. However, due to the lack of blocking inhibitors or antibodies of BIN2, we could not demonstrate this directly, which is a limitation of our study. Yet, the observed, extensive phosphorylation changes in BIN2 and STIM1 upon platelet activation *via* GPVI or PAR, among which several predicted PKC-dependent phosphorylation sites, is compatible with a highly regulated ORAI1-BIN2-STIM1 pathway.

Both our inhibitor studies and the kinase prediction of regulated phospho-sites in BIN2 and STIM1 point to a combined role of several isoforms, at least PKCβ and PKCθ (lower expressed), and likely other PKC isoforms as well in suppression of the concluded ORAI1-BIN2-STIM1 pathway. In other words, it seems that in response to platelet agonists, phosphorylation events by multiple activated PKC isoforms are responsible for constraining the SOCE process. Which of the several PKC-dependent phosphorylations is responsible for the suppression of ORAI1-mediated Ca^{2+} entry still needs to be studied.

In the past, a negative regulation by PKC of agonist-induced [Ca^{2+}]i rises has been seen in platelets and other cell types, but this was not linked to Ca^{2+} entry. Thus, diacylglycerol analogs (which can activate PKC) were found to suppress thapsigargin-induced [Ca^{2+}]i rises in rabbit neutrophils (33). In platelets and cell lines, it was suggested that specifically PKCβ antagonizes thrombin receptor-induced Ca^{2+} fluxes (34, 35), which is in line with our results. In 2010, Harper and colleagues used diacylglycerol analogs to distinguish between Ca^{2+} entry mechanisms in platelets and concluded that PKCθ restricts a store-*in*dependent pathway (36). The same authors reported that oleoylacetyl glycerol induced a negative regulation of PAR1-dependent Ca^{2+} fluxes along with phosphatidylserine exposure (37). In 2013, the Kunapuli laboratory demonstrated that in human (but not mouse) platelets, the PKCβ isoform induced hyperphosphorylation of Syk and PLCγ2, thereby enhancing GPVI-mediated responses (38). In light of the current findings, such data may also be interpreted as PKC-mediated suppression *via* the ORAI1-BIN2-STIM1 axis.

Platelet PKC activity is commonly known to be essential in integrin activation, secretion and aggregate formation (21, 39, 40). The current finding of a negative role of PKC isoforms in ORAI1-dependent platelet procoagulant activity hence places this kinase in a key position to regulate the balance of pro-aggregatory and procoagulant platelets. Currently, ORAI1 channel antagonists are proposed as a treatment option in cases of exacerbated Ca^{2+} signaling, such as observed in pulmonary arterial hypertension (41). Our data suggest that such antagonists may also influence platelet-dependent thrombotic events.

Experimental procedures

Materials

Thrombin was obtained from Enzyme Research Laboratories. Thrombin receptor-activating peptide SFLLRN (TRAP6) and AYPGKF were from Bachem (Bubendorf, Switzerland). Cross-linked collagen-related peptide (CRP) came from CambCol (Cambridge, UK). Fura-2 acetoxymethyl ester was from Invitrogen, pluronic F-127 from Molecular Probes (Eugene, OR, USA). Compounds RO318425 (bisindolylmaleimide X), 2-aminoethyl diphenylborinate (2- APB), phorbol myristate acetate (PMA), PKCθ inhibitor (PKCθ-IN) and LY379196 (PKCβ-IN) were from Sigma-Aldrich (St Louis, MO, USA); PRT-060318 from Bio- Connect. Convulxin and GF109203X (bisindolylmaleimide I) came from Enzo Life Sciences (Lausen, Switzerland). Horm-type collagen (dissolved in 0.1 M acetic acid) was obtained from Nycomed (Hoofddorp, the Netherlands). From Merck-Calbiochem (Darmstadt, Germany) came the non-maleimide compound Gö6976; acalabrutinib was from Abcam. Thapsigargin was from Santa Cruz Biotechnology (Dallas, TX, USA); fluorogenic thrombin substrate Z-Gly-Gly-Arg-aminomethylcoumarin (ZGGR-AMC) from Bachem. Recombinant tissue factor (Innovin) came from Siemens Healthineers. Other materials were from sources, described before (42).

Characterization of pharmacological compounds

Panel comparison using 302 purified protein kinases (43) provided for the PKC antagonists GF109203X (bisindolylmaleimide I), Gö6976, and PKCβ-IN percentual inhibitory activities, as indicated in Table 1. Compound Gö6976 is also known to interfere with tyrosine kinase Syk (26). Relative

inhibitory activities of RO318425 (bisindolylmaleimide X) and PKCθ-IN were obtained from earlier papers (21, 22) (Table 1). Acalabrutinib acts as a selective blocker of platelet tyrosine kinase Btk (44). The compound rottlerin was not used as a PKCδ inhibitor, given its abundant side effects.

Patients and blood collection

The included healthy male and female blood donors had not taken anti-platelet medication for at least 10 days prior to blood donation. All donors had given full informed consent according to the Helsinki Declaration. The studies were approved by the Medical Ethics Committee of Maastricht University and the local Ethics Committee of the University Medical Center Mainz (Study No. 837.302.12; 25.07.12; FF109/2015). Approval excluded the recording of donor characteristics. Patients with immune deficiency and a deleterious mutation in ORAI1 (R91W, homozygous) or STIM1 (R429C, R/C heterozygous), along with healthy day control subjects were collected at the Department of Pediatrics and Adolescent Medicine of the Medical Center, University of Freiburg. All blood was taken by venipuncture and collected into 3.2% sodium citrate. Platelet counts were measured with a Sysmex XN-9000 analyzer (Sysmex).

Preparation of Fura-2-loaded platelets

Platelet-rich plasma (PRP) and washed platelets were obtained from citrated blood samples, as described (45). Pelleted platelets were first resuspended in Hepes buffer pH 6.6 (10 mM Hepes, 136 mM NaCl, 2.7 mM KCl, 2 mM MgCl2, 5.5 mM glucose, and 0.1% BSA). Washed platelets were obtained by a second centrifugation step in the presence of apyrase (1 U/ml) and 1:15 vol/vol ACD. After resuspension in Hepes buffer pH 7.45, the cells were loaded with Fura-2 acetoxymethyl ester (3 μM) and pluronic (0.4 μg/ml) (16). Final platelet resuspension after another wash step was in Hepes buffer pH 7.45 at the count of 2×10^8/ml.

Calibrated changes in $[Ca^{2+}]i$

Calibrated nanomolar rises in $[Ca^{2+}]i$ of Fura-2-loaded platelets were measured in 96-well plates using a FlexStation three robot (Molecular Devices, San Jose, CA, USA), as described (25). Briefly, samples of 200 μl (2×10^8 platelets/ml) per well were pretreated with indicated inhibitor (10 min) at 37 °C, and supplemented with 1 mM CaCl2 or 0.1 mM EGTA. During dual-wavelength recording of fluorescence changes, a selected agonist (20 μl) was added by automated pipetting, which resulted in diffusion-limited mixing (46). Parallel calibration wells contained Fura- 2-loaded platelets with 0.1% Triton-X-100 in the presence of either 1 mM CaCl2 or 1 mM EGTA/Tris, for determining Rmax and Rmin values. Duplicate time traces were generated of nanomolar $[Ca^{2+}]i$ concentrations, and were floating point averaged to obtain the curve parameters: basal level (nM), peak value (nM), area under the activation curve (nM × s), and 600 s end level (nM) (16). For measurements of Fura-2-loaded patient platelets, calibrated ratio fluorometry was performed in single cuvettes (47).

Platelet procoagulant activity

Agonist-induced phosphatidylserine exposure of washed platelets (5×10^7/ml in Hepes buffer pH 7.45) was performed in the presence of 2 mM CaCl2, as described (28). Platelets were activated for 5 to 10 min with convulxin in the presence or absence of PKC inhibitor and then labeled with FITC-annexin A5 (0.25 μg/ml). Fluorescence analysis of 5000 events per sample was done with an Accuri C6 flow cytometer. Events were gated for SSC/FSC signals of platelets. Percentages of phosphatidylserine-positive platelets were determined from F1 fluorescence levels (unstimulated platelets set at 2%).

Thrombin generation

For calibrated thrombin generation (30), samples of PRP in 96-well plates were pre-incubated with selected inhibitor (10 min, 37 °C), and mixed with thrombin substrate solution (ZGGR-AMC) and trigger solution (tissue factor 0.1 PM, 11 mM CaCl2 and 5.5 mM MgCl2). Thrombin generation curve parameters were obtained as before (30).

Label-free platelet phosphoproteome analysis

Purified washed platelets from three donors (5×10^8/ml) in the presence of 1 mM CaCl2 were stimulated with CRP (10 μg/ml) or thrombin (4 nM) or kept untreated. Activations were stopped with one volume of lysis buffer at peaks of the Ca^{2+} signal, *i.e.* after 3 min for CRP or 30 s for thrombin. Platelets were then lysed, cysteines were reduced, free sulfhydryl groups were alkylated, and proteins were digested with trypsin under strictly regulated conditions, such as described in the supplementary methods. Details of the mass spectrometry of the label-free digests as well as the spectral analyses are also provided in the supplementary methods.

Identified peptides were restrained to BIN2, STIM1, or ORAI1 for high confidence with FDR <1% at the PSM level, and a search engine rank of 1. This resulted in BIN2 (Q9UBW5) in 125 phosphopeptides, STIM1 (Q13586) in 35 phosphopeptides, and for ORAI1 (Q96D31) in one phosphopeptide. The peptides included carbamidomethyl derivatives as well as monophospho, biphospho, triphospho, and quatrophospho peptides, all for serine and threonine residues. Normalized abundance values (NAVs) from equal phosphosites across all peptides were rationed *versus* the control condition per sample and donor and expressed as log2 fold changes after CRP or thrombin stimulation (see Datafile S1). Protein structural information was obtained from UniProt/KB cards.

TMT-based platelet phosphoproteome analysis

Purified washed platelets (5.0×10^8/ml) from one healthy donor were activated in the presence of 1 mM CaCl2 with CRP (10 μg/ml, three or 30 min) or thrombin (4 nM, 30 s or 30 min) or were kept untreated (duplicate samples), as above. After stopping reactions with SDS and PhosStop, lysed samples were subjected to quality checks, cysteine reduction, free sulfhydryl alkylation, and trypsin digestion with TMT (tandem mass tag) 10-plex stable isotope labels, as described before (48) with

details in the supplementary methods. Lookup searches were confined to high-confidence phosphopeptides (FDR < 1%) from BIN2 (Q9UBW5), STIM1 (Q13586) or ORAI1 (Q96D31). This resulted in 48, 27, and 3 phosphopeptides, respectively (Datafile S1). Per individual sample phosphopeptide, log2 fold changes *versus* controls were calculated from values of TMT pools.

Prediction of PKC isoform phosphorylation

Identified peptides with assigned phospho-sites were subjected to a search in PhosphoSitePlus, using the recent kinase library for substrate specificities of 303 serine/threonine protein kinases, including five relevant PKC isoforms (32). Amino acid residues with a positive prediction (log2 score) for all five PKCα/β/δ/ε/θ isoforms were for BIN2: S256/S257 (0.25–2.17) and S285 (0.61–1.69). Positive prediction scores for PKCα/β/δ comprised the phospho-sites S429/S430 (3x, 0.70–1.15), T447 (2x, 0.40–0.57), S451 (3x, 0.19–1.44) and S458 (2x, 0.79–1.28). For STIM1, positive prediction scores for PKCα/β/δ/ε/θ comprised S512 (1.16–2.54), and S567 (2x, 0.36–1.45). Prediction scores for other phospho-sites in peptides were negative for ≥4 PKC isoforms. See Datafile S1. Genetic variants of BIN2, STIM1, and BIN2 phospho-sites were checked in ClinVar (ncbi.nlm.nih.gov/clinvar).

Statistics

Data are expressed as mean ± SD. GraphPad Prism 8 was used for analysis. Statistical differences in comparison to the control condition were evaluated by the non-parametric Mann-Whitney U-test. Significance was defined as $p < 0.05$.

Data availability

All experimental data are contained within the manuscript. Raw mass spectrometry data and Proteome Discoverer search results are deposited in ProteomeXchange repository, identifier PXD0487897.

Supporting information—This article contains supporting information (31, 48-53).

Authors contributions—I. P., C. S., J. Z., P. Z., and A. S. methodology; I. P., F. A. S., J. Z., P. Z., J. W. M. H., B. Z., F. S., and N. J. A. M. investigation; I. P., F. A. S., C. S., P. Z., J. S. R., F. S., and M. J. E. K. formal analysis; I. P., C. S., J. Z., K. J., P. Z., J. W. M. H., A. S., J. S. R., and N. J. A. M. data curation; C. S., P. Z., and J. W. M. H. writing–original draft; C. S. and B. Z. validation; K. J., J. W. M. H., F. S., and M. J. E. K. writing–review & editing; K. J., J. W. M. H., A. S., and M. J. E. K. supervision; K. J. J. W. M. H., and A. S. funding acquisition. J. W. M. H. and B. Z. resources, J. W. M. H. and F. S. conceptualization.

Funding and additional information—JZ acknowledges bursary support from the China Scholarship Council (CSC) 201909370052. PZ and CS are supported by the European Union's Horizon 2020 research and innovation program under the Marie Sklodowska-Curie grant agreement TICARDIO no. 813409. PZ and CS are enrolled in a joint PhD program with the Universities of Mainz and Maastricht.

Conflicts of interest—The authors declare the following financial interests/personal relationships which may be considered as potential competing interests: JWMH is scientific advisor for Synapse Research Institute Maastricht. The other authors report no relevant conflicts of interest.

Abbreviations—The abbreviations used are: BIN2, bridging integrator 2; BSA, bovine serum albumin; CRP, collagen-related peptide; GPVI, glycoprotein VI; PCK, protein kinase C; PMA, phorbol myristate acetate; PRP, platelet-rich plasma; TRAP6, thrombin receptor-activating peptide-6.

References

1. Braun, A., Varga-Szabo, D., Kleinschnitz, C., Pleines, I., Bernder, M., Austinat, M., *et al.* (2009) Orai1 (CRACM1) is the platelet SOC channel and essential for pathological thrombus formation. *Blood* **113**, 2056–2063
2. Varga-Szabo, D., Braun, A., and Nieswandt, B. (2011) STIM1 and Orai1 in platelet function. *Cell Calcium* **50**, 70–278
3. Mammadova-Bach, E., Nagy, M., Heemskerk, J. W., Nieswandt, B., and Braun, A. (2019) Store-operated calcium entry in thrombosis and thrombo-inflammation. *Cell Calcium* **77**, 39–48
4. Gilio, K., van Kruchten, R., Braun, A., Berna-Erro, A., Feijge, M. A., Stegner, D., *et al.* (2010) Roles of platelet STIM1 and Orai1 in glycoprotein VI- and thrombin- dependent procoagulant activity and thrombus formation. *J. Biol. Chem.* **285**, 23629–29638
5. Van Kruchten, R., Braun, A., Feijge, M. A., Kuijpers, M. J., Rivera-Galdos, R., Kraft, P., *et al.* (2012) Antithrombotic potential of blockers of store-operated calcium channels in platelets. *Arterioscler Thromb. Vasc. Biol.* **32**, 1717–1723
6. Fahrner, M., Muik, M., Derler, I., Schindl, R., Fritsch, R., Frischauf, I., *et al.* (2009) Mechanistic view on domains mediating STIM1-Orai coupling. *Immunol. Rev.* **231**, 99–112
7. Volz, J., Kusch, C., Beck, S., Popp, M., Vögtle, T., Meub, M., *et al.* (2020) BIN2 orchestrates platelet calcium signaling in thrombosis and thrombo-inflammation. *J. Clin. Invest.* **130**, 6064–6079
8. Versteeg, H. H., Heemskerk, J. W., Levi, M., and Reitsma, P. H. (2013) New fundamentals in hemostasis. *Physiol. Rev.* **93**, 327–358
9. Fernandez, D. I., Kuijpers, M. J., and Heemskerk, J. W. (2020) Platelet calcium signaling by G- protein coupled and ITAM-linked receptors regulating anoctamin-6 and procoagulant activity. *Platelets* **32**, 1–9
10. Bergmeier, W., Oh-hora, M., McCarl, C. A., Roden, R. C., Bray, P. F., and Feske, S. (2009) R93W mutation in Orai1 causes impaired calcium influx in platelets. *Blood* **109**, 6875–6878
11. Nagy, M., Mastenbroek, T. G., Mattheij, N. J., de Witt, S., Clemetson, K. J., Kirschner, J., *et al.* (2018) Variable impairment of platelet functions in patients with severe, genetically linked immune deficiencies. *Haematologica* **103**, 540–549
12. Feske, S., Gwack, Y., Prakriya, M., Srikanth, S., Puppel, S. H., Tanasa, B., *et al.* (2006) A mutation in Orai1 causes immune deficiency by abrogating CRAC channel function. *Nature* **441**, 179–185
13. Fuchs, S., Rensing-Ehl, A., Speckmann, C., Bengsch, B., Schmitt-Graeff, A., Bondzio, I., *et al.* (2012) Antiviral and regulatory T cell immunity in a patient with stromal interaction molecule 1 deficiency. *J. Immunol.* **188**, 1523–1533
14. Borsari, O., Piga, D., Costa, S., Govoni, A., Magri, F., Andrea, A., *et al.* (2018) Stormorken syndrome caused by a p.R304W STIM1 mutation: the first Italian patient and a review of the literature. *Front. Neurol.* **9**, 859
15. Boehm, J., and Laporte, J. (2018) Gain-of-function mutations in STIM1 and ORAI1 causing tubular aggregate myopathy and Stormorken syndrome. *Cell Calcium* **76**, 1–9
16. Cheung, H. Y. F., Zou, J., Tantiwong, C., Fernandez, D. I., Huang, J., Ahrends, R., *et al.* (2023) High-throughput assessment identifying major

platelet Ca^{2+} entry pathway via tyrosine kinase- linked and G protein-coupled receptors. *Cell Calcium* **112**, 102738
17. Munnix, I. C. A., Harmsma, M., Giddings, J. C., Collins, P. W., Feijge, M. A. H., Comfurius, P., *et al.* (2003) Store-mediated calcium entry in the regulation of phosphatidylserine exposure in blood cells from Scott patients. *Thromb. Haemost.* **89**, 687–695
18. Huang, J., Swieringa, F., Solari, F. A., Provenzale, I., Grassi, L., De Simone, I., *et al.* (2021) Assessment of a complete and classified platelet proteome from genome-wide transcripts of human platelets and megakaryocytes covering platelet functions. *Sci. Rep.* **11**, 12358
19. Konopatskaya, O., Gilio, K., Harper, M. T., Zhao, Y., Cosemans, J. M., Karim, A. Z., *et al.* (2009) PKCa regulates platelet granule secretion and thrombus formation in mice. *J. Clin. Invest.* **119**, 399–407
20. Nagy, B., Bhavaraju, K., Getz, T., Bynagari, Y. S., Kim, S., and Kunapuli, S. P. (2009) Impaired activation of platelets lacking protein kinase C-theta isoform. *Blood* **113**, 2557–2567
21. Gilio, K., Harper, M. T., Cosemans, J. M., Konopatskaya, O., Munnix, I. C., Prinzen, L., *et al.* (2010) Functional divergence of platelet protein kinase C (PKC) isoforms in thrombus formation on collagen. *J. Biol. Chem.* **285**, 23410–23419
22. Strehl, A., Munnix, I. C., Kuijpers, M. J., van der Meijden, P. E., Cosemans, J. M., Feijge, M. A., *et al.* (2007) Dual role of platelet protein kinase C in thrombus formation: stimulation of pro-aggregatory and suppression of procoagulant activity in platelets. *J. Biol. Chem.* **282**, 7046–7055
23. Makhoul, S., Kumm, E., Zhang, P., Walter, U., and Jurk, K. (2020) The serine/threonine protein phosphatase 2A (PP2A) regulates Syk activity in human platelets. *Int. J. Mol. Sci.* **21**, 8939
24. Zhang, P., Solari, F. A., Heemskerk, J. W., Kuijpers, M. J., Sickmann, A., Walter, U., *et al.* (2023) Differential regulation of GPVI-induced Btk and Syk activation by PKC, PKA and PP2A in human platelets. *Int. J. Mol. Sci.* **24**, 7776
25. Fernandez, D. I., Provenzale, I., van Groningen, J., Tullemans, B. M., Veninga, A., Dunster, J. L., *et al.* (2022) Ultra-high throughput Ca^{2+} response patterns in platelets to distinguish between ITAM-linked and G-protein coupled receptor activation. *iScience* **25**, 103718
26. Getz, T. M., Mayanglambam, A., Daniel, J. L., and Kunapuli, S. P. (2011) Go6976 abrogates GPVI-mediated platelet functional responses in human platelets through inhibition of Syk. *J. Thromb. Haemost.* **9**, 608–610
27. Rosado, J. A., Meijer, E. M., Hamulyak, K., Novakova, I., Heemskerk, J. W., and Sage, S. O. (2001) Fibrinogen binding to the integrin αIIbβ3 modulates store-mediated calcium entry in human platelets. *Blood* **97**, 2648–2656
28. Van Kruchten, R., Mattheij, N. J., Saunders, C., Feijge, M. A., Swieringa, F., Wolfs, J. L., *et al.* (2013) Both TMEM16F-dependent and TMEM16F-independent pathways contribute to phosphatidylserine exposure in platelet apoptosis and platelet activation. *Blood* **121**, 1850–1857
29. Mattheij, N. J. A., Braun, A., van Kruchten, R., Castoldi, E., Pircher, J., Baaten, C. C. F. M. J., *et al.* (2016) Survival protein anoctamin-6 controls multiple platelet responses including phospholipid scrambling, swelling and protein cleavage. *FASEB J.* **30**, 727–737
30. Sun, S., Campello, E., Zou, J., Konings, J., Huskens, D., Wan, J., *et al.* (2023) Crucial roles of red blood cells and platelets in whole blood thrombin generation. *Blood Adv.* **21**, 6717–6731
31. Hogrebe, A., von Stechow, L., Bekker-Jensen, D. B., Weinert, B. T., Kelstrup, C. D., and Olsen, J. V. (2018) Benchmarking common quantification strategies for large-scale phosphoproteomics. *Nat. Commun.* **9**, 1045
32. Johnson, J. L., Yaron, T. M., Huntsman, E. M., Kerelsky, A., Song, J., Regev, A., *et al.* (2023) An atlas of substrate specificities for the human serine/threonine kinome. *Nature* **613**, 759–766
33. Shibata, K., Kitayama, S., Morita, K., Shirakawa, M., Okamoto, H., and Dohi, T. (1994) Regulation by protein kinase C of platelet-activating factor- and thapsigargin- induced calcium entry in rabbit neutrophils. *Jpn. J. Pharmacol.* **66**, 273–276
34. Xu, Y., and Ware, J. A. (1995) Selective inhibition of thrombin receptor-mediated Ca^{2+} entry by protein kinase C beta. *J. Biol. Chem.* **270**, 23887–23890
35. Kawasaki, T., Ueyama, T., Lange, I., Feske, S., and Saito, N. (2010) Protein kinase C-induced phosphorylation of Orai1 regulates the intracellular Ca^{2+} level via the store- operated Ca^{2+} channel. *J. Biol. Chem.* **285**, 25720–25730
36. Harper, M. T., and Poole, A. W. (2010) Protein kinase C theta negatively regulates store- independent Ca^{2+} entry and phosphatidylserine exposure downstream of glycoprotein VI in platelets. *J. Biol. Chem.* **285**, 19865–19873
37. Harper, M. T., and Poole, A. W. (2011) PKC inhibition markedly enhances Ca^{2+} signaling and phosphatidylserine exposure downstream of protease-activated receptor-1 but not protease-activated receptor-4 in human platelets. *J. Thromb. Haemost.* **9**, 1599–1607
38. Buitrago, L., Bhavanasi, D., Dangelmaier, C., Manne, B. K., Badolia, R., Borgognone, A., *et al.* (2013) Tyrosine phosphorylation on spleen tyrosine kinase (Syk) is differentially regulated in human and murine platelets by protein kinase C isoforms. *J. Biol. Chem.* **288**, 29160–29169
39. Harper, M. T., and Poole, A. W. (2010) Diverse functions of protein kinase C isoforms in platelet activation and thrombus formation. *J. Thromb. Haemost.* **8**, 454–462
40. Zou, J. (2022) Reversible platelet integrin αIIbβ3 activation and thrombus instability. *Int. J. Mol. Sci.* **23**, 12512
41. Masson, B., Le Ribeuz, H., Sabourin, J., Laubry, L., Woodhouse, E., Foster, R., *et al.* (2022) Orai1 inhibitors as potential treatments for pulmonary arterial hypertension. *Circ. Res.* **131**, e102–e119
42. Gilio, K., Munnix, I. C., Mangin, P., Cosemans, J. M., Feijge, M. A., van der Meijden, P. E., *et al.* (2009) Non-redundant roles of phosphoinositide 3-kinase isoforms α and β in glycoprotein VI- induced platelet signaling and thrombus formation. *J. Biol. Chem.* **284**, 33750–33762
43. Anastassiadis, T., Deacon, S. W., Devarajan, K., Ma, H., and Peterson, J. R. (2011) Comprehensive assay of kinase catalytic activity reveals features of kinase inhibitor selectivity. *Nat. Biotechnol.* **29**, 1039–1045
44. Tullemans, B. M., Heemskerk, J. W., and Kuijpers, M. J. (2018) Acquired platelet antagonism: off-target antiplatelet effects of malignancy treatment with tyrosine kinase inhibitors. *J. Thromb. Haemost.* **16**, 1686–1699
45. Feijge, M. A., Ansink, K., Vanschoonbeek, K., and Heemskerk, J. W. (2004) Control of platelet activation by cyclic AMP turnover and cyclic nucleotide phosphodiesterase type-3. *Biochem. Pharmacol.* **67**, 1559–1567
46. Jooss, N. J., De Simone, I., Provenzale, I., Fernandez, D. I., Brouns, S. L., Farndale, R. W., *et al.* (2019) Role of platelet glycoprotein VI and tyrosine kinase Syk in thrombus formation on collagen-like surfaces. *Internatl J. Mol. Sci.* **20**, e2788
47. Van der Meijden, P. E., Feijge, M. A., Swieringa, F., Gilio, K., Nergiz-Unal, R., Hamulyak, K., *et al.* (2012) Key role of integrin αIIbβ3 signaling to Syk kinase in tissue factor-induced thrombin generation. *Cell Mol Life Sci* **69**, 3481–3492
48. Swieringa, F., Solari, F. A., Pagel, O., Beck, B., Faber, J., Feijge, M. A., *et al.* (2020) Impaired iloprost-induced platelet inhibition and phosphoproteome changes in patients with confirmed pseudohypoparathyroidism type Ia, linked to genetic mutations in GNAS. *Sci. Rep.* **10**, 11389
49. Provenzale, I., Solari, F. A., Schönichen, C., Brouns, S. L., Fernandez, D. I., Kuijpers, M. J., *et al.* (2024) Endothelial regulation of platelet activation and signaling: endothelial effects on platelet phosphoproteome. *FASEB J* **38**, e23468
50. Burkhart, J. M., Schumbrutzki, C., Wortelkamp, S., Sickmann, A., and Zahedi, R. P. (2012) Systematic and quantitative comparison of digest efficiency and specificity reveals the impact of trypsin quality on MS-based proteomics. *J Proteomics* **75**, 1454–1462
51. Solari, F. A., Mattheij, N. J., Burkhart, J. M., Swieringa, F., Collins, P. W., Cosemans, J. M., *et al.* (2016) Combined quantification of the global proteome, phosphoproteome, and proteolytic cleavage to characterize altered platelet functions in the human Scott syndrome. *Mol Cell Proteomics* **15**, 3154–3169
52. Beck, F., Geiger, J., Gambaryan, S., Solari, F. A., Dell'Aica, M., Loroch, S., *et al.* (2017) Temporal quantitative phosphoproteomics of ADP stimulation reveals novel central nodes in platelet activation and inhibition. *Blood* **129**, e1–e12
53. Post, H., Penning, R., Fitzpatrick, M. A., Garrigues, L. B., Wu, W., MacGillavry, H. D., *et al.* (2017) Robust, sensitive, and automated phosphopeptide enrichment optimized for low sample amounts applied to primary hippocampal neurons. *J Proteome Res* **16**, 728–737